# Low-Cost Rapid Prototyping of High-Resolution Printed Liquid-Metal Circuits and Devices

Kareem S. Elassy, *Student Member, IEEE*, Jubeyer Rahman, Anthony W. Combs, David G. Garmire, *Senior Member, IEEE*, Wayne A. Shiroma, *Senior Member, IEEE*, and Aaron T. Ohta\*, *Senior Member, IEEE* 

Abstract—Patterning liquid-metal circuits and devices at high resolution requires expensive equipment. This work demonstrates a low-cost method to rapidly prototype liquid-metal patterns for flexible and stretchable electronics. The setup consists of a programable syringe pump connected to a 3D printer with polymeric tubing. The liquid-metal flow rate and printing speed are simultaneously adjusted to obtain high-resolution printed features of 35-µm lines, with 105-µm spacing between the lines. A proof-of-concept circuit is demonstrated on a polymeric substrate to show the compatibility of the technique with flexible surfaces.

#### I. INTRODUCTION

Printed electronics have been used for a variety of devices and circuits such as sensors [1], transistors [2], biological sensors [3], solar-cell electrodes [4], and antennas [5]. Many of these printed circuits and devices are implemented using conductive nanoparticle inks [6]. Patterns made with nanoparticle inks can crack after the solvent evaporates, reducing the conductivity of the printed features [7]. Electronic circuits can also be created by liquid metal (LM) [8]–[12], which does not crack like nanoparticle inks; additionally, it can heal cracked conductive paths [13]. The printing of LM is a rapid prototyping method that can create conductive patterns that are also compatible with flexible substrates.

A challenge to printing LM is attaining high-resolution features using low-cost printers. An elastomer printhead on a three-axis Cartesian robot can deposit individual droplets of LM on an elastomer substrate [14], but the droplet size of 340  $\mu$ m limited the resolution of the printed patterns. The printhead also needed to be inked before depositing each droplet. Another setup for printing LM costs about \$15,000, with a reported resolution of ~50  $\mu$ m [15]. Other researchers created a droplet generator capable of creating 10- $\mu$ m LM droplets [16], resulting in a minimum printed feature size of 48  $\mu$ m.

In this work, we report a new method of rapidly prototyping high-resolution LM patterns using a low-cost setup. We integrated a programmable syringe pump (KDS- 210 or NE-300) with plastic 3D printer (MakerGear M2); the setup costs about \$2500. The synchronization between the LM flow rate and printing speed has been optimized to achieve high-resolution LM patterns. Different needle sizes have been used to print diverse line widths ranging from 200 μm down to 35 μm. The bed temperature has been optimized promote the wetting of printed LM (PDMS) polydimethylsiloxane and polyethylene terephthalate (PET) substrates. The printed LM, Galinstan, is a non-toxic gallium-based LM alloy with an electrical conductivity of  $3.4 \times 10^6$  S/m [17].

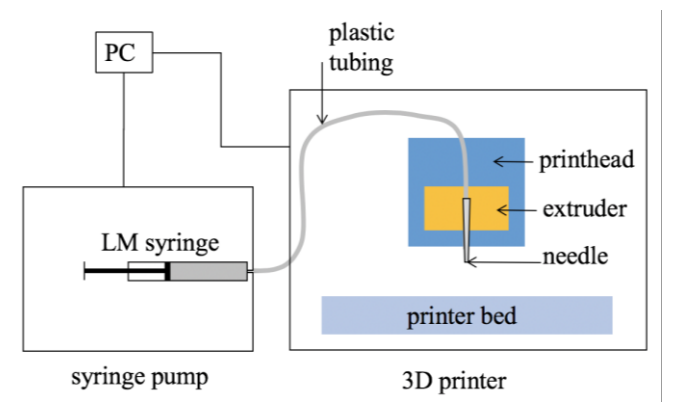


Fig. 1 Schematic diagram for the printing setup

#### II. DESIGN, SETUP, AND PRINTING PARAMETERS

# A. Design

The first step in the design and fabrication process was using Autodesk 123D software to design the drawing file exported as stereo-lithography file extension (STL). The STL file was then imported into the slicing software (Cura) in which the layers settings (layer height and shell thickness) were edited to ensure that the output file would include a single pass of the pattern. Cura software produces a G code which dictates the trajectory and stops of the printhead.

Research is supported in part by the National Science Foundation (grant FCCS-1807896)

K.S. Elassy<sup>1</sup>, J. Rahman, A.W. Combs, W.A. Shiroma and A.T. Ohta are with the Electrical Engineering Department, University of Hawai'i at Mānoa, 2540 Dole St., Honolulu, HI 96822, USA. (email: elassy@hawaii.edu; jubeyer@hawaii.edu; combsa@hawaii.edu shiromaw@hawaii.edu; aohta@hawii.edu)

\*Corresponding author: A. T. Ohta, aohta@hawaii.edu

<sup>1</sup>also with Center of Excellence, Arab Academy for Science, Technology and Maritime Transport, Smart Village P.O. Box 12577, Egypt

D.G. Garmire was with the University of Hawai'i at Mānoa, HI 96822 USA. He is now with University of Michigan at Ann Arbor 1301 Beal Ave, Ann Arbor, MI 48105 (email: dgarmire@umich.edu)

#### B. Setup

Fig. 1 shows a schematic diagram for the printing setup. The syringe pump (Fig. 2a) can be controlled either manually or by LabView code (developed by National Instruments). Polymer tubing (Tygon) with inner diameters of 0.25, 0.51, or 0.76 mm was attached to the syringe. The other end of the tubing was inserted into the hot-end channel of the 3D printer after the nozzle was removed (Fig. 2b). A needle of size 21, 23, 25, or 34 gauge was inserted and sealed into the end of the tubing of the 3D printer.



(a)

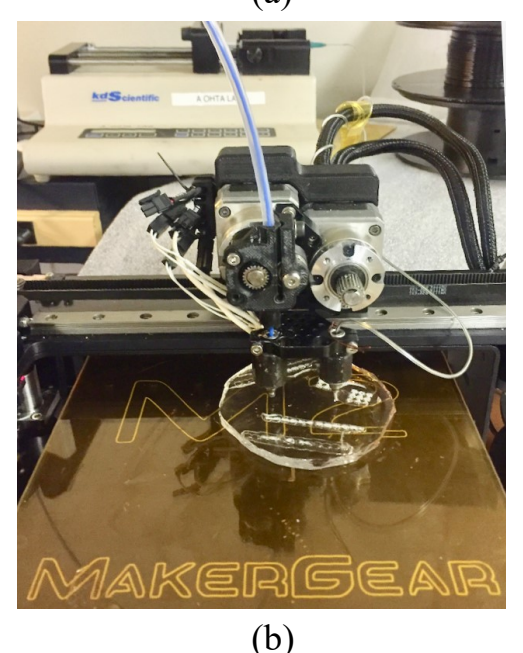


Fig. 2 Fabrication setup (a) syringe pump with 1-mL syringe of LM, (b) 3D printer with tubing coming from syringe pump and inserted into the printhead

# B. Printing Parameters

The fluid flow rate from the syringe pump was within 0.025 to 0.1 mL/min, and synchronized to the 1 mm/s x-y printing speed controlled by the printing software. The syringe pump and the 3D printer must be synchronized carefully to start ejecting LM once the printhead receives the command to start moving to create the pre-designed pattern. The syringe pump was started 2 s before running the G code to move the printhead. This allowed the pressure to

accumulate inside the tubing to eject LM as the printhead starts to follow the coded trajectory.

#### III. RESULTS AND DISCUSSION

Following the procedures described above, a series of test structures were produced to demonstrate the technique. Fig. 3 shows the LM patterns achieved by 2D printing LM on PDMS substrate with a thickness of 0.5 cm. The bed temperature of the printer was varied from 25 °C to 120 °C to enhance LM adhesion with the substrate.

### A. Optimizing Printing Conditions

The goal of this work was to print the finest possible features while preserving the continuity and edge quality of the printed lines. First, a wide needle was used until the proper flow rate, bed temperature, and printing speed was determined for continuous printed LM features. Then, the needle gauge was decreased while adjusting the flow rate and bed temperature to determine the printing parameters resulting in the smallest possible feature size. Table 1 shows the printing parameter sets used. Fig. 3a shows a spiral shape with an outer diameter of 10 cm and 0.7-mm linewidth, achieved using a 21-gauge needle tip with a 0.1 mL/min flow rate and a 100 °C bed temperature. A significant number of bulges and inconsistencies were found in the LM pattern due to Rayleigh instability [17].

TABLE I. PRINTING PARAMETER SETS

Parameters Set #	Printing Condition		
	Flow rate (mL/min)	Platen temperature (℃)	Needle size (gauge)
a	0.1	100	21
b	0.05	100	23
c	0.025	120	25

Decreasing the flow rate to 0.05 mL/min at the same bed temperature eliminated the LM bulges with a 21-gauge needle. The same flow rate and bed temperature were used with a 23-gauge needle to produce a printed 0.5-mm linewidth (Fig. 3b). It was observed that only one section of the pattern had excess LM, and this was eliminated with a 0.025 mL/min flow rate at the same bed temperature (100 °C). After that, the printing parameters of a 0.025 mL/min flow rate and 100 °C bed temperature were used with a 25-gauge needle, but the printed LM pattern tended to coalesce rather than sticking to the PDMS substrate, introducing discontinuities and excess LM in the pattern. Better results showing a consistent 0.3-mm linewidth were achieved with the 25-gauge needle by adjusting the bed temperature to 120 °C (Fig. 3c).

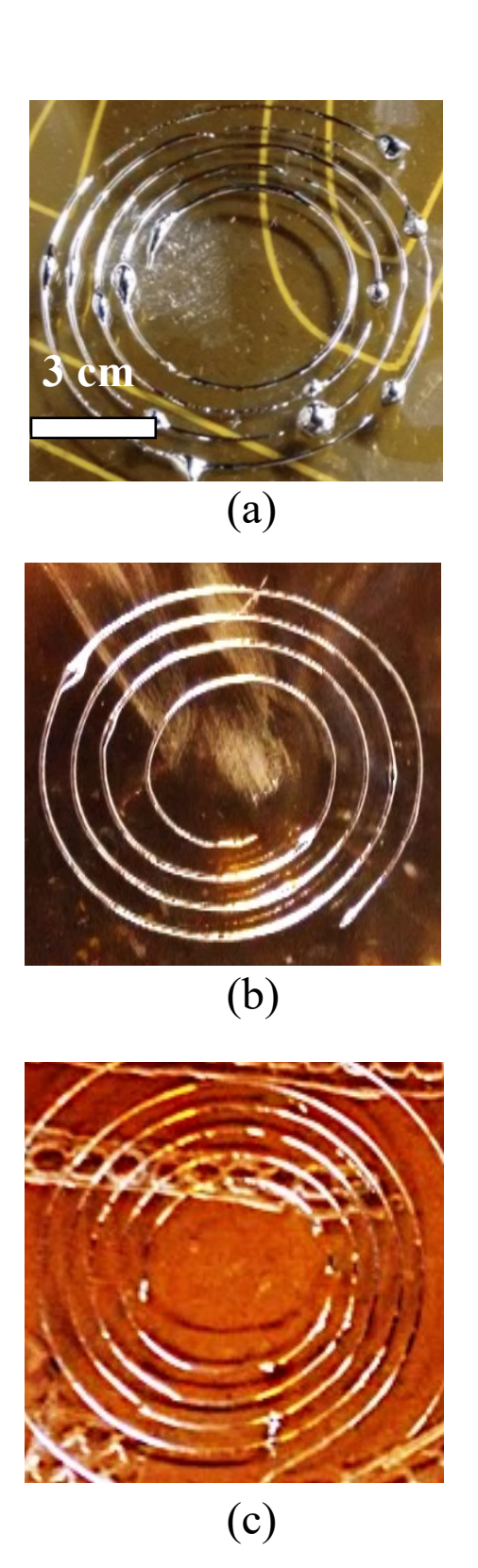


Fig. 3 Spiral LM pattern with an extrusion rate of:
(a) 0.1 mL/min at 100 °C print bed temperature using 21-gauge needle
(b) 0.05 mL/min at 100 °C print bed temperature using 23-gauge needle
(c) 0.025 mL/min at 120 °C print bed temperature using 25-gauge needle

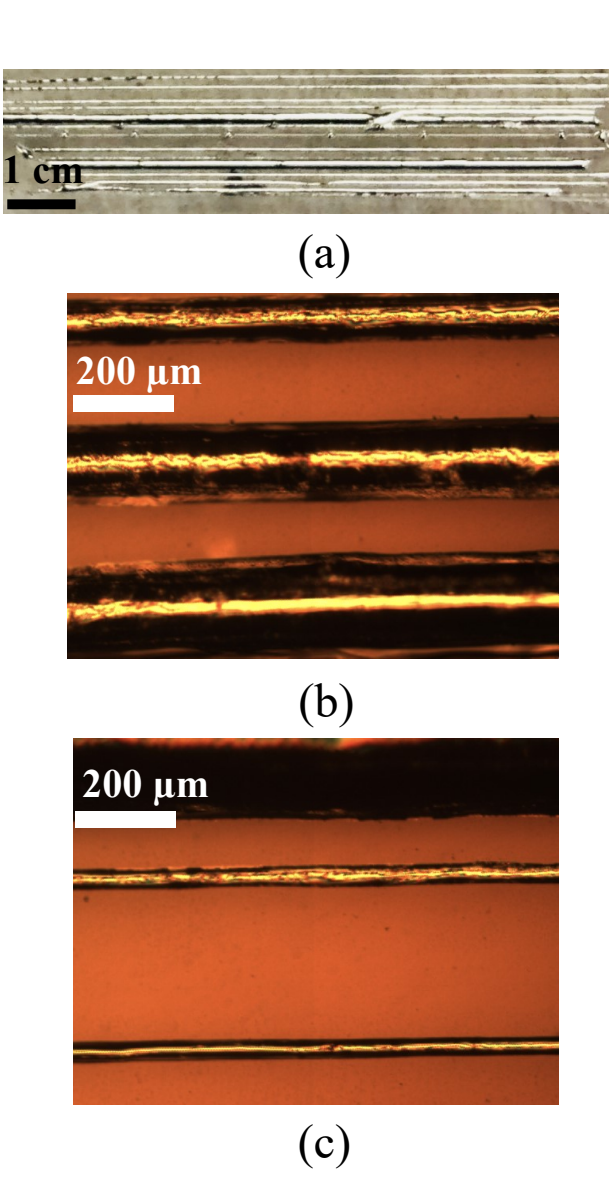


Fig. 4 Printed LM lines on a PET substrate, printed at 100 °C bed temperature (a) printed LM lines (b) lines with widths of 100 to 200  $\mu m$ , (c) lines with a width of 35  $\mu m$ 

# B. High Resolution Printing

The highest resolution of printed lines was approximately 35  $\mu m.$  It was achieved using the 34-gauge needle tip for lines printed on a PET substrate with a thickness of 100  $\mu m$  (Fig. 4c). A bed temperature of 100 °C was enough to stick the printed LM on the PET substrate as its small thickness, compared to the 0.5-cm thickness of PDMS, allowed better heat transfer from the substrate bottom to top surface. The spacing between the lines was 105  $\mu m$ , which is the minimum step size (100  $\mu m$ ) that can be reached by the 3D printer's X-Y motors.

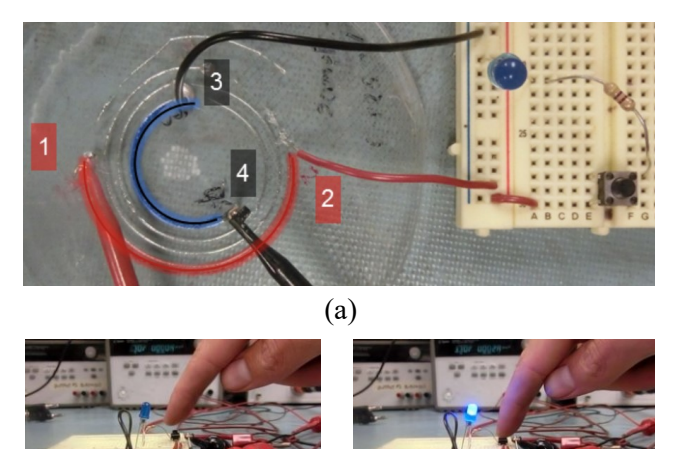


Fig. 5 Proof-of-concept circuit demonstration with push-button switch (a) circuit with printed LM as wires, (b) push-button switch open, LED off, (c) push-button switch closed, LED on

(c)

# C. Proof-of-Concept Circuit

(b)

A proof-of-concept circuit was built to demonstrate the electrical continuity of the LM circuitry after it had been patterned and encased in PDMS. Four ports were used to connect two LM "wires" to the rest of the circuit (labeled in Fig. 5a). The positive DC probe was connected to port 1, and current flowed through the Galinstan to port 2. The current entered the part of the circuit on a breadboard, which consisted of a push-button switch, a 1.5-k $\Omega$  resistor, and a blue LED. The current left the components on the breadboard and returned to the patterned LM circuitry at port 3. The current flowed through Galinstan to port 4, which was connected to the negative DC probe.

### IV. CONCLUSION

The proposed technique has provided a successful alternative to high-cost LM printers to rapidly prototype high resolution LM patterns. A programmable syringe pump was connected to a 3D printer to extrude LM instead of plastic filament. The fluid flow rate was optimized and synchronized with the printer speed, as well as the bed temperature, to achieve high-resolution printed LM lines of 35  $\mu m$  width. The spacing of the printed lines was 105  $\mu m$ , limited by the X-Y motor step size of the printer.

#### REFERENCES

- A. Al-Halhouli, H. Qitouqa, A. Alashqar, and J. Abu-Khalaf, "Inkjet printing for the fabrication of flexible/stretchable wearable electronic devices and sensors," *Sens. Rev.*, vol. 38, no. 4, pp. 438–452, Sep. 2018
- [2] G. Zhang, P. Zhang, H. Chen, and T. Guo, "Modification of polymer gate dielectrics for organic thin-film transistor from inkjet printing," *Appl. Phys.* A, vol. 124, no. 7, p. 481, Jul. 2018.
- [3] S. K. Tuteja, C. Ormsby, and S. Neethirajan, "Noninvasive label-free detection of cortisol and lactate using graphene embedded screenprinted electrode," *Nano-Micro Lett.*, vol. 10, no. 3, p. 41, Jul. 2018.
- [4] K. Hwang, Y. S. Jung, Y. J. Heo, F. H. Scholes, S. E. Watkins, J. Subbiah, D. J. Jones, D. Y. Kim, and D. Vak, "Toward large scale roll-to-roll production of fully printed perovskite solar cells," *Adv. Mater.*, vol. 27, no. 7, pp. 1241–1247, 2015.

- [5] H. Liu, J. Wang, and X. Luo, "Flexible and compact AMC based antenna for WBAN applications," in 2017 IEEE Antennas and Propagation Society International Symposium, Proceedings, 2017, vol. 2017-Janua, pp. 587–588.
- [6] M. Grouchko, A. Kamyshny, C. F. Mihailescu, D. F. Anghel, and S. Magdassi, "Conductive inks with a 'built-in' mechanism that enables sintering at room temperature," ACS Nano, vol. 5, no. 4, pp. 3354–3359, 2011.
- [7] J. S. Kang, H. S. Kim, J. Ryu, H. T. Hahn, S. Jang, and J. W. Joung, "Inkjet printed electronics using copper nanoparticle ink," J. Mater. Sci. Mater. Electron., vol. 21, no. 11, pp. 1213–1220, Nov. 2010.
- [8] J. L. Melcher, K. S. Elassy, R. C. Ordonez, C. Hayashi, A. Ohta, and D. Garmire, "Spray-on liquid-metal electrodes for graphene fieldeffect transistors," *Micromachines*, vol. 10, no. 1, p. 54, Jan. 2019.
- [9] K. S. Elassy, T. K. Akau, W. A. Shiroma, S. Seo, and A. T. Ohta, "Low-cost rapid fabrication of conformal liquid-metal patterns," *Appl. Sci.*, vol. 9, no. 8, p. 1565, Apr. 2019.
- [10] G. B. Zhang, R. C. Gough, M. R. Moorefield, K. S. Elassy, A. T. Ohta, and W. A. Shiroma, "An electrically actuated liquid-metal gain-reconfigurable antenna," *Int. J. Antennas Propag.*, vol. 2018, pp. 1–7, 2018.
- [11] M. U. Baig, K. S. Elassy, A. Host-Madsen, A. Ohta, W. Shiroma, and A. Nosratinia, "Managing interference through discrete modulation and liquid metal antennas," in 2018 IEEE 88th Vehicular Technology Conference, Chicago, IL, Aug. 2018.
- [12] A. M. Watson, T. F. Leary, K. S. Elassy, A. G. Mattamana, M. A. Rahman, W. A. Shiroma, and A. T. Ohta, "Physically reconfigurable RF liquid electronics via Laplace barriers," *IEEE Trans. Microw. Theory Tech.*, vol. 67, no. 12, Dec. 2019.
- [13] G. Li, X. Wu, and D. W. Lee, "A Galinstan-based inkjet printing system for highly stretchable electronics with self-healing capability," *Lab Chip*, vol. 16, no. 8, pp. 1366–1373, 2016.
- [14] A. Tabatabai, A. Fassler, C. Usiak, and C. Majidi, "Liquid-phase gallium-indium alloy electronics with microcontact printing," *Langmuir*, vol. 29, no. 20, pp. 6194–6200, 2013.
- [15] C. Ladd, J. H. So, J. Muth, and M. D. Dickey, "3D printing of free standing liquid metal microstructures," *Adv. Mater.*, vol. 25, no. 36, pp. 5081–5085, 2013.
- [16] T. Liu, P. Sen, and C. J. Kim, "Characterization of nontoxic liquid-metal alloy Galinstan for applications in microdevices," J. *Microelectromech. Syst.*, vol. 21, no. 2, pp. 443–450, Apr. 2012.
- [17] M. P. Brenner, J. Eggers, K. Joseph, S. R. Nagel, and X. D. Shi, "Breakdown of scaling in droplet fission at high Reynolds number," *Phys. Fluids*, vol. 9, no. 6, pp. 1573–1590, Jun. 1997.